NUMERICAL SIMULATION OF IRON OXIDE CONCRETION FORMATION ON EARTH AND MARS.

S. Sirono[1], T. Shibata[1], N. Katsuta[2] and H. Yoshida[3], [1]Graduate School of Earth and Environmental Sciences, Nagoya University (Furo-tyo, Tikusa-ku, Nagoya 464-8601, Japan), [2] Faculty of Education, Gifu University (Yanagido 1-1, Gifu city, Gifu 501-1193, Japan), [3]Nagoya University Museum (Furo-tyo, Tikusa-ku, Nagoya 464-8601 Japan).

Introduction: Iron oxide concretions are found on Earth and Mars in sedimentary rocks. On Earth, in particular, concretions are commonly observed in eolian formations, such as Jurassic Navajo Sandstone, Utah, USA [1,2], and those found in the Gobi desert, Mongolia [3]. Although it is known that the formation conditions of the iron oxide concretions are affected by the paleoclimate of these regions, quantitative modeling providing thickness of an iron rim still requires further development. The key property or quantifying factor of an iron oxide concretion is the ratio between the thickness of the rim and the radius of the concretion. The comparison between the measured ratios of natural samples and the simulation results enables us to constrain the groundwater conditions when iron oxide concretions were formed.

Outline of the model: Inside a layer of a sandstone, a spherical region filled with calcite is formed by precipitation. The calcite is surrounded by groundwater containing Fe^{3+} and H^+. Dissolution of calcite decreases $[H^+]$, inducing precipitation of $Fe(OH)_3$ around the surface of the calcite sphere and a rim of $Fe(OH)_3$ is formed. Both H^+ and Fe^{3+} ions are transported from the outer region through diffusion.
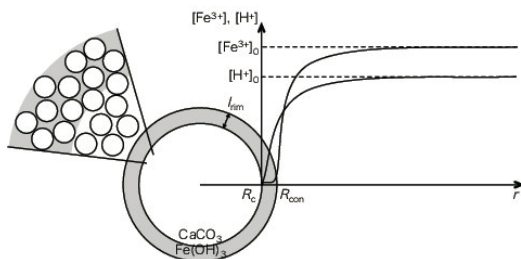

Figure 1: Schematic of the model of iron rim formation. The gray region represents $Fe(OH)_3$ filling the pore spaces between sandgrains. Hydrogen and iron ions diffuse to the surface of the calcite sphere, where precipitation of $Fe(OH)_3$ proceeds.

Drying of $Fe(OH)_3$ rim. In natural samples, iron oxide fills almost totally the pore spaces between sandgrains inside the iron rim. The remaining porosity is less than 10%. It should be noted that $Fe(OH)_3$ precipitates as colloidal particles and cannot fill the pore spaces between sandgrains without drying. It has been well known that a colloidal particle migrate with the water-air interface as drying proceeds [4]. Drying proceeds from outside when the water surface is lower than the precipitation after draining. The high volume fraction of $Fe(OH)_3$ around the calcite sphere delays the drying compared to the surrounding region. When drying proceeds from outside of the precipitation, the water surface moves toward the calcite sphere. As a result, $Fe(OH)_3$ colloidal particles migrate to the surface of the calcite sphere (Fig. 2).

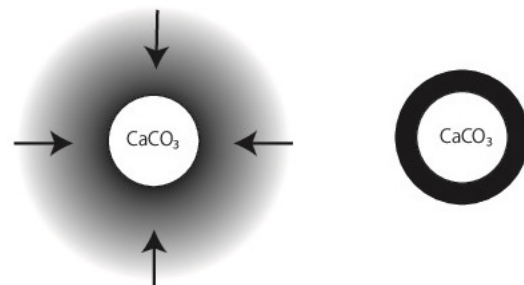*Figure 2: Drying of $Fe(OH)_3$ precipitate. As drying proceeds, colloidal particles migrate to the surface of the calcite sphere.*

Numerical results: At the beginning of the simulation, precipitation occurs outside the calcite sphere. Then precipitation of $Fe(OH)_3$ proceeds inward as the calcite sphere dissolves (Fig.3).
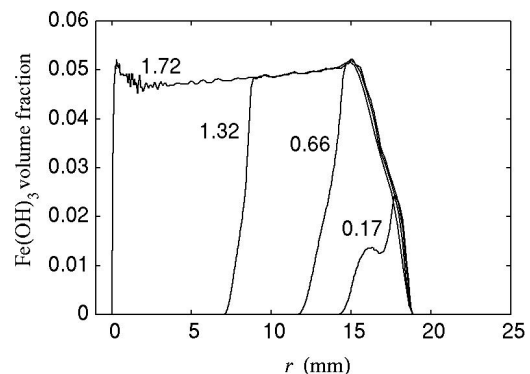

Figure 3: Distribution of $Fe(OH)_3$ precipitation as a function of the distance from the center of the calcite sphere. The volume fraction is unity if $Fe(OH)_3$ totally fills the pore spaces between sandgrains. The numbers attached to the curves are the time in yr. The initial conditions of ions are given by $[Fe^{3+}]_0=10^{-2}$ mol L^{-1} and $[H^+]_0=10^{-2}$ mol L^{-1}.

The volume fraction of $Fe(OH)_3$ occupying pore space is at most 0.05 (Fig. 3), which cannot explain the typical volume fraction of iron oxide inside pore space 0.8-0.9 [3]. The dissolution of calcite sphere completes in 1.72 yr.

If we assume that the migration of $Fe(OH)_3$ proceeds completely through the drying, the thickness of the rim can be estimated from Fig. 3 as a function of time. Figure 4 displays the evolution of the concretion rim/radius ratio as a function of the normalized time (with respect to the time required to the total dissolution of the calcite sphere).
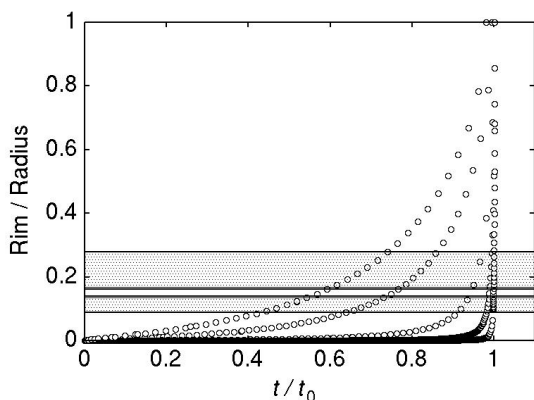

Figure 4: The ratio between the thickness of the rim and concretion radius as a function of the normalized time. Circles are the simulation results. The gray regions are the ratios obtained from the natural samples. From top to bottom, the initial iron concentration is $[Fe^{3+}]_0 = 10^{-1.5}, 10^{-2}, 10^{-3}, 10^{-4},$ *and* 10^{-5} mol L^{-1} *with a fixed hydrogen concentration* $[H^+]_0 = 10^{-2}$ mol L^{-1}.

From Fig. 4, the time when the dissolution is finished can be constrained from the natural samples. If the concentration of iron ion $[Fe^{3+}]$ is high, the time required to attain the observed ratio is short. If the iron concentration is low, the suitable time range for natural samples is limited only around $t/t_0 = 1$, indicating that the probability is low and difficult to explain. Therefore, the iron concentration should be substantially high such that $[Fe^{3+}]_0 > 10^{-2}$ mol L^{-1}.
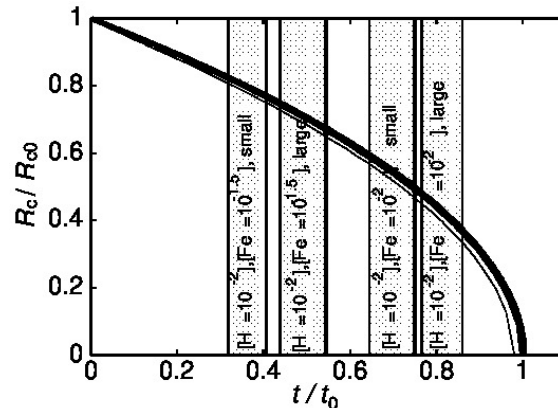

Figure 5: The ratio between the concretion radius and the initial radius of the calcite sphere as a function of the normalized time. The gray regions are the ranges obtained from Fig. 4 for different concentrations.

From the range of t/t_0, the original size of the calcite sphere can be estimated from Fig.5. The gray regions are the estimated size range in which the natural samples are consistently explained (Fig. 4). It can be seen that the original size of the calcite sphere is larger than twice of that of the observed natural samples of concretions if the concentration of iron ion is low.

In the outcrops, the distance between iron oxide concretion is longer than ten concretion radii [1]. The distance between concretions should be longer than the ratio determined from Fig. 5, otherwise the initial calcite spheres overlap. Therefore, the iron concretions found in Utah can be formed through dissolution of calcite sphere followed by precipitation of $Fe(OH)_3$ if the concentration of iron ion is higher than 10^{-2} mol L^{-1}, taking account of the duration of the dissolution (Fig. 4). On the other hand, blueberries in Meridiani planum have much shorter distance [6] between them that than in Utah, and difficult to explain by the scenario investigated in this study.

References: [1] Chan, M. A. et al. (2004) *Nature, 429,* 731–734. [2] Loope D. B. et al. (2010) *Geology, 38,* 999-1002. [3] Yoshida et al. (2018) *Sci. Adv.*4: eearu0872, [4] DeNovio et al. (2004) *Vadose Zone J.,* 3 338–351. [5] Squyres et al. (2004) *Science,* 306 1698–1703. [6] Weitz et al. (2006) *JGR,* 111 E12S04.